International Electrotechnical Commission
Technical Committee 77 - Electromagnetic Compatibility
Subcommittee 77B - High-Frequency Phenomena

Contribution to: Joint Working Group on Overvoltage Control
From: François D. Martzloff

Revisiting reality checks on the surge environment

In our quest for data on the frequency of occurrence and level of threat of overvoltages, we should not overlook some "reality checks" that can be applied to proposals for characterizing the surge environment. In the white paper (Martzloff/London)1 of July 1995, four examples of reality checks were cited to inject some perspective in the process and avoid excessive conservatism in assessing the need for high current requirements for SPDs installed in buildings. Two of these raised questions from the AJWG, which I will attempt to clarify in this follow-up white paper.

Questions:

[1] Forcing a large current with steep front toward an SPD installed at the far end of a circuit may require such a high voltage that the connections at the near end of the cable will flashover, limiting the stress applied to the far-end SPD. Some members of the AJWG felt that the model presented was over-simplified and might not represent reality.

[2] Incandescent light bulbs do not easily survive surges in excess of 1200-1500 V. Thus, unless we have strong evidence that many light bulbs fail before their normal expected rated life, we must conclude that the occurrence of a surge above 1500 V is not a frequent event. The AJWG asked whether such data could be applied to light bulbs used in the 240-V world. Our U.K. colleagues expressed interest in performing similar tests on 240-V rated bulbs.

Responses:

[1] We present the results of modeling ***and*** tests, validating each other. A varistor was included at the far end, and the computations were conducted with lumped-parameters as well as with transmission-line models. The conclusions presented in London are confirmed. Some useful information was obtained concerning the need to watch out for blind spots and avoid intuitive reasoning in SPD applications.

[2] The offer to perform the tests under the same experimental conditions, with bulbs supplied by our U.K. colleagues, did not make any such bulbs arrive. We performed a limited test on a few bulbs that we happened to have available; the results are consistent with the behaviour of 120 V bulbs. We also report other findings based on further tests with 120-V rated bulbs that have implications on failure mechanisms of other appliances.

These two re-visited examples, developed in cooperation with my colleagues of the Power Electronics Applications Center, are discussed in more detail in the following sections. The limitation on driving voltage for steep current fronts was modeled by Arshad Mansoor and the corresponding measurements were recorded by Kermit Phipps. The additional incandescent light bulb tests were made by Doni Nastasi.

SURGE CURRENT LIMITATION BY WIRING INDUCTANCE AND CLEARANCES WITHSTAND

Please refer to the original London paper for the background of this reality check. The questions raised by the AJWG were as follows:

1. Is the model an oversimplification because it does not include a varistor at the far end ?
2. Why were transmission line effects that occur in reality not taken into consideration ?
3. Could interaction between the upstream network and the branch circuit affect the circuit behaviour ?

To answer these three questions, we first performed a test on real-world circuits elements, then proceeded to apply the EMTP code to model the circuit behaviour, using the lumped parameter model (used in the London paper), as well as the transmission line model, each being available in the EMTP code. The postulate was made that the surge current used in the test and the modeling is not the textbook 8/20 but results from a current source and is shaped by the upstream network into the surge that our surge generator could deliver at the sending end of our real-world circuit. After the results of the tests and the modeling have been found to validate each other, one can always run the model with some other waveform, such as the textbook 8/20 if that is what one wishes for comparisons, for instance.

1. Modeling of the varistor

First, the varistor to be connected at the far end was tested to determine its I-V response and verify that the model used for this highly nonlinear component was adequate to simulate its behavior in the circuit when connected at the far end. Figure 1 shows the test circuit used for making that measurement and Figure 2 shows the recording obtained for a particular setting of the surge generator. This generator was the KeyTek 711 with P7 wave-shaping output network.

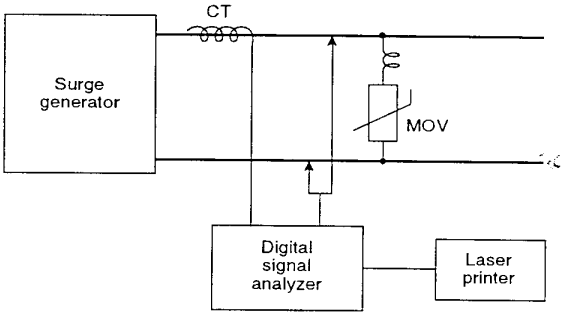

Figure 1 - Test circuit for determination of the I-V characteristics of the varistor

The varistor used in these tests was a 20-mm diameter disc, rated 130 V rms (200 V at 1 mA d.c.). The inductance shown in series with the varistor is not a deliberate addition of a real component, but the representation of the coupling between the loop where the surge current flows and the voltage measurement loop formed by the varistor leads and the two probes used for the differential measurement. That inductance is included in the model as a discrete series inductance, with a value of 0,5 μH selected to emulate the observed voltage at the point of measurement -- which is not the "pure" varistor voltage, as discussed in the narrative of Figure 2.

Figure 3 shows the result of modeling the circuit of Figure 1 for an impinging current surge corresponding to the real-world current surge recorded in Figure 2. The equation for the modeling was developed by Arshad Mansoor as a damped sine wave with a multiplier term $[1-e^{(-t)}]$ that avoids the problem of non-zero derivative at the origin discussed in (Martzloff/London)02:

$$4200.0*\sin(0{,}126t)*e^{(-t/26{,}1)}*[1-e^{(-t)}] \qquad \text{(t in microseconds)}$$

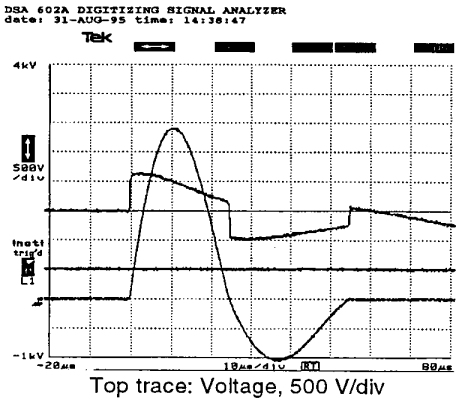

Top trace: Voltage, 500 V/div
Center trace: inactive
Bottom trace: Current, 500 A/div
Sweep: 10 µs/div

Figure 2 - Real-world recording

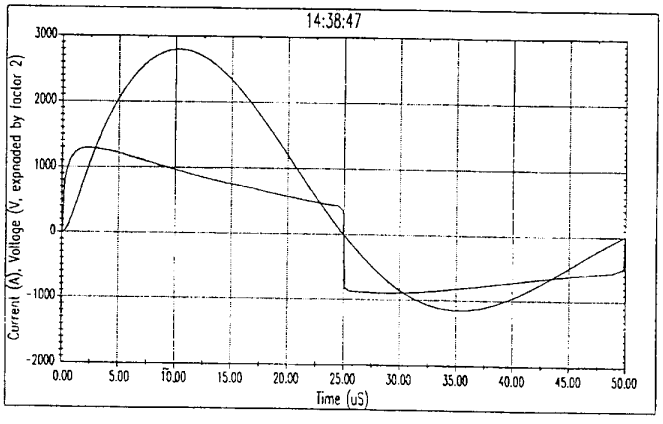

Figure 3 - Modeling the circuit of Figure 1 with the impinging current set to match that of Figure 2

Inspection of Figures 2 and 3 clearly shows the agreement of real-world measurement and model, including the effect of the parasitic inductance in series with the pure varistor: at the time of $di/dt = 0$ (current peak), the "true" varistor voltage is measured; before the peak, the positive di/dt adds a spurious voltage to the recording, and after the peak, the negative di/dt subtracts the spurious voltage.

The model used in the simulation for the varistor is derived from the published varistor I-V characteristic (general shape and slope of the curve) with one specific point defined by the "true" varistor voltage read from the oscillogram of Figure 2 at the point of zero $L \times di/dt$ contribution. In turn, this varistor model will be used in the modeling of a varistor connected at the end of a branch circuit, as discussed in the following measurements/simulations.

2. Varistor installed at the end of a branch circuit

The object of this test/model is to determine the voltage at the sending end necessary to drive a stated current down the branch circuit into an SPD connected at the end of the branch circuit. Instead of the simplified case of a branch circuit with far-end shorted presented in London (to allow normalized results), this case is more complex as it includes both the linear effect of branch circuit inductance and nonlinear effect of the varistor.

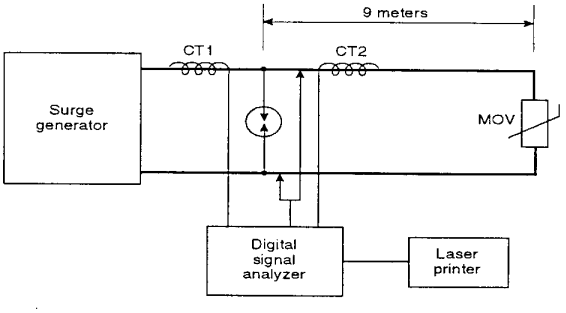

Figure 4 - Test circuit for determination of the voltage necessary at the sending end to drive a given current into the far-end SPD

The circuit of Figure 4 shows the varistor characterized by the test and modeling of the preceding paragraphs, connected at the end of a "branch circuit" consisting of two conductors, #12 AWG (2 mm^2). The first current transformer monitors the total current impinging at the sending end. The second current transformer monitors the current flowing toward the far end, that will be imposed on the varistor. The clearances at the sending end, for instance the clearances existing in a service-entrance panel, are represented by a discrete gap that will be set to produce sparkover at some given voltage during the test as well as in the model.

Figure 5 shows the recording obtained for the circuit of Figure 4, with the surge generator left at the same setting as that used for Figure 2. The gap setting was such that no sparkover occurred for the sending-end voltage developed in this test.

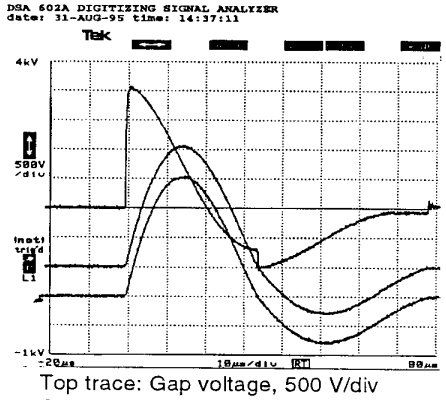

Top trace: Gap voltage, 500 V/div
Center trace: Total current, 500 A/div
Bottom trace: MOV current, 500 A/div
Sweep: 10 µs/div

Figure 5 - Real-world recording of sending-end voltage with gap set for no sparkover

From inspection of this Figure 5 and comparison with the recording of Figure 2, some observations are appropriate:

The addition of the inductance of the 9 meters of branch circuit changes the load on the surge generator, reducing the current peak from 2.8 kA in Figure 2 to 2 kA in Figure 5.

The two current traces of Figure 5 are identical. Since there is no current diverted by the gap, the current in the branch circuit is the same as the current delivered by the surge generator.

Another effect of the added inductance is the increase in the time from origin to the first current zero, 33 µs in Figure 5, compared to 25 µs in Figure 2 In the subsequent model, that change of the impinging current surge is taken into consideration by modifying the current equation as follows:

$$5355.0*\sin(0{,}095t)*e^{(-t/26{,}1)}*[1-e^{(-t)}]$$

Turning to the modeling, Figures 6 and 7 show the waveforms of the impinging current, as defined by the equation cited above, and the resulting voltage at the sending end. To address the concern expressed at the London meeting of the AJWG, the EMTP modeling was done with the lumped circuit parameter model, as were all the other models, but that of Figure 7 which was obtained by the transmission line model which is available in the EMTP code. Inspection of the two figures reveals no difference in the results. The only difference is in the consumption of computing time: with the transmission line model, the computation time step has to be significantly shorter (0.02 µs in this case) than the travel time for the reflections, while in the case of the lumped model, the interval can be longer (0.1 µs in this case). The result is that the simulation of Figure 6 took 43 seconds on a 486-based PC, compared to 263 seconds for Figure 7. Thus, the lumped elements model is perfectly adequate to represent the reality, and performing a transmission-line analysis is an unnecessary consumption of computing time.

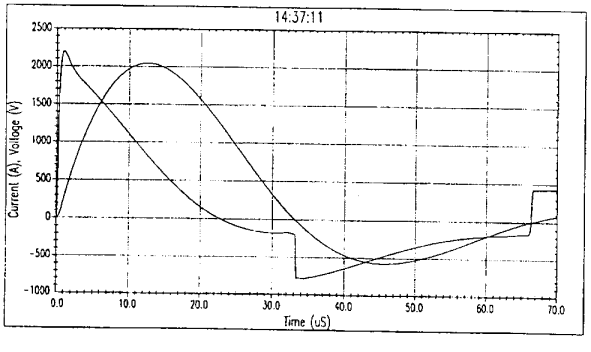

Figure 6 - Lumped parameters model

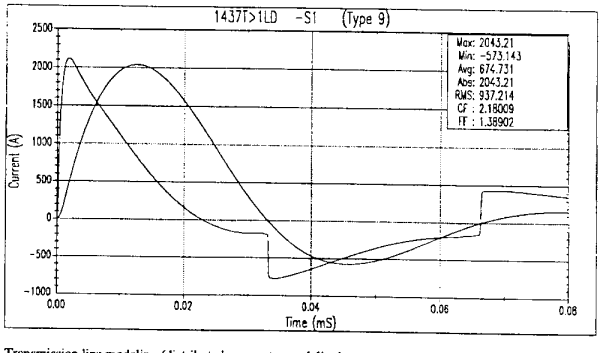

Transmission line modeling (distributed parameter modeling)
L = .5µH/m, C = 50pF/m corresponds to Z= 100 and v = 200m/µsec

Figure 7 - Transmission line model

Having established that the model is an adequate representation of reality, we can now use the model to compute a set of voltages at the sending end resulting from imposing any given current into a branch circuit of any given length. Table 1 below shows the results of such computations for the waveform of Figures 5, 6 and 7 (where the rise time is the significant factor).

Table 1
Voltage (kV) necessary to drive a current of the peak value shown (columns) and rise time of 10 µs into a branch circuit of length as shown (rows) terminated with a 130-V rated varistor

Length \ Peak	2 kA	3 kA	5 kA	7 kA	10 kA
10 m	2.3	3.3	5.2	7.2	10.1
30 m	5.8	8.5	13.9	19.4	27.0
50 m	9.3	13.7	22.7	31.6	45.0

Now equipped with this tool, we will be happy to provide to the AJWG similar parametric data for any waveform that the AJWG would select to illustrate examples of cascade coordination and the limitation of the current postulated in SPD specifications for the far-end SPD.

The London presentation did not include computations of the current in the varistor that continues to flow, even after the gap has sparked over, as a result of the energy stored in the branch circuit inductance during the time it took the gap to sparkover. Of course, the longer the branch circuit, the greater the inductance for storing energy. If the postulated scenario is that of a current source (unlike our tests where we had only a surge generator which is not a perfect current source), then i^2 remains the same. Therefore, there is some interest in assessing the current waveform and total energy deposition imposed onto the far-end varistor as a function of branch circuit length. After demonstrating the validation of the model in the next figures, we will report the results of a parametric set of energy into the varistor as a function of line length.

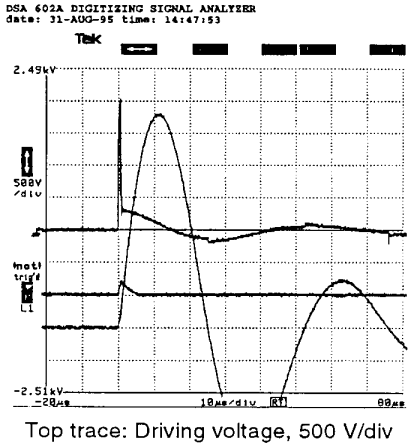

Top trace: Driving voltage, 500 V/div
Center trace: MOV current, 500 A/div
Bottom trace: Total current, 500 A/div
Sweep: 10 µs/div

Figure 8 - Voltages and currents with gap set to sparkover at 2 kV

Figure 8 shows the real-world recording of the situation that develops for a "clearance" sparkover of 2 kV. This relatively low value, compared to the 6 kV to 10 kV level that we might expect from typical low-voltage wiring devices, is made necessary for the test case where only 9 meters of branch circuit were considered, and the setting of the surge generator maintained at the same nominal 3 kA short-circuit current setting. The object, of course, is to demonstrate that the clearances are likely to flashover, as indicated by the progressively higher values of the necessary driving voltage shown in Table 1.

Sparkover of the gap occurs at 1 µs, presumably while the current in the branch circuit was initially rising at a rate similar to that shown in Figure 5. After sparkover, the current delivered by the surge generator is the sum of the current in the gap and the current into the branch circuit. Its peak (3.2 kA) is greater than those of Figures 2 and 5 because the generator does not need to overcome the varistor voltage that reduced the voltage available for driving the current in Figure 5. Note that the driving voltage (top trace) after sparkover contains some additional voltage induced in the measuring loop in a manner similar to the voltage measurement of Figure 2 (true gap voltage at the peak of the current).

For the sake of simplifying the modeling, only one waveform was postulated to be applied to the circuit, derived from the observed waveform of Figure 8. In the model, designed to represent a constant current source, the impinging current waveform does not change when the clearance flashes over. In the test shown by Figure 8, we can expect that the current would jump to a higher level after the gap sparkover, as recorded by the instrumentation. We chose that value to represent the post-sparkover condition which occupies most of the trace. The difference between the pre- and post-sparkover is small enough in the case of Figure 8 to allow this simplification. Thus, the equation used for modeling the case of the sparkover is :

$$4800.0*\sin(0{,}126t)*e^{(-t/26{,}1)}*[1-e^{(-t)}]$$

Figures 9, 10, and 11 show the results obtained by the model for voltages and current in the circuit.

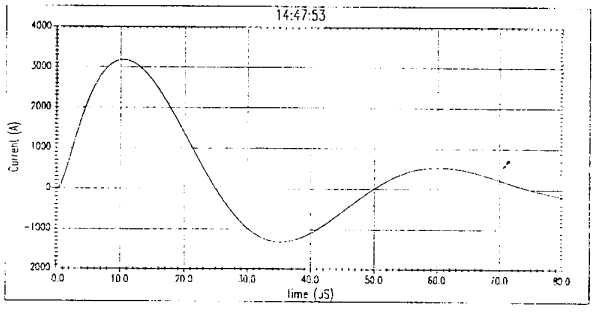

Figure 9 - Total current delivered by the surge generator in the case of gap sparkover

Figure 9 is the current, as defined by the equation shown above, with its smooth, soft toe produced by the $[1-e^{(-t)}]$ multiplier.

Comparing this current to the current waveform of Figure 8, good correspondence is noted for the rise time, peak amplitude, time to first zero between the two current waveforms. Close examination of the initial rise of the current in Figure 8 does not reveal a conspicuous discontinuity at the time of gap sparkover, justifying the simplification discussed above.

The waveforms shown in Figures 10 and 11 have an expanded scale, compared to Figure 8, that gives a better resolution for the gap voltage and current in the varistor. There is good correspondence between these two and the two traces of Figure 8.

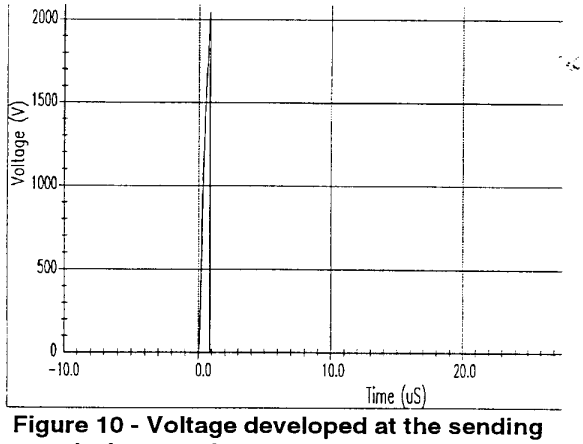

Figure 10 - Voltage developed at the sending end when gap is set to sparkover at 2 kV

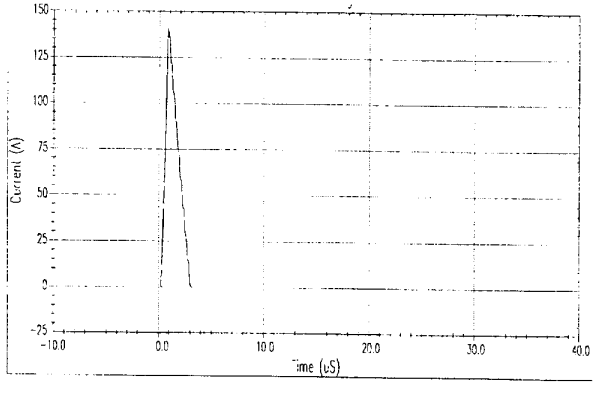

Figure 11 - Current in varistor before and after sparkover of the gap

As mentioned above, we can expect that the energy deposited in the far-end varistor for a given impinging surge will be influenced by the length of the branch circuit. Using the model developed and validated according to Figure 11, this energy can be readily computed. In the case described by Figures 8, 9, 10 and 11, the gap sparkover voltage was set at 2 kV so that sparkover could indeed occur for the current available from the real-world generator. Now that we are in the (validated) model world, we can set the gap (clearance) sparkover voltage at a level more typical of the flashover of clearances, say 6 kV. In the example reported below, we will keep the same three values of branch circuit length and perform the computations for the same five values of impinging current. Of course, we have the possibility of assessing the energy for a wide range of parameters if needed. Table 2 shows the energy deposited in the far-end varistor for these combinations of branch circuit length and peak current values, for the applied current waveform of Figure 5.

Table 2
Energy deposited into a 130-V rated far-end varistor as a function of the branch circuit length shown (rows) and current peak (columns) of waveform shown in Figure 5

Length \ Peak	2 kA	3 kA	5 kA	7 kA	10 kA
10 m	**21.5 J**	**35.2 J**	1.1 J	431 mJ	175 mJ
30 m	273 mJ	102 mJ	43 mJ	26 mJ	15 mJ
50 m	55 mJ	31 mJ	15 mJ	12 mJ	8 mJ

The results shown in Table 2 merit close examination as they reveal some counter-intuitive trends: we might have expected that with higher impinging current values, the resulting energy deposited in the varistor would be higher. Likewise, we might have expected that for a longer branch circuit, the greater inductance would store more energy, ultimately to be deposited in the varistor. In fact, the opposite occurs. There is also the interesting fact that the first two low-current, short-line cases (bold face type in the table) produce large energy deposition, compared to all the other cases. Actually, the explanation that follows is simple and might be anticipated (in particular with hindsight, illustrating that intuition is a hazardous process when dealing with nonlinear circuit components).

Starting with the second observation (more joules at lower threat levels), we have a beautiful illustration of the ***blind spot*** effect: with 10 meters of circuit and the lower current levels, the driving voltage at the clearance is not sufficient to cause flashover, so that all the energy has to go to the far-end varistor. At the higher treat level of 5 kA, the voltage produced in the inductance of 10 meters of line, added to the varistor voltage, is sufficient to sparkover the 6 kV gap, relieving the varistor from further involvement beyond that of discharging the energy stored in the 10-m long line.

Turning now to the first two observations, that higher current or greater inductance result in less stress, this apparent paradox is caused by the fact that with the higher values of di/dt and of L drive the voltage at the clearance more quickly to the flashover point. The build-up of energy in the line inductance is thus shut-off earlier so that the current level in the line reached at that point is lower and, in spite of the greater inductance, the stored energy $\frac{1}{2} L i^2$ is lower for higher applied current peaks and longer branch circuits. Thus, the lower energy numbers going down the columns and left to right in the rows of the table are perfectly understandable.

In conclusion, I hope that this reality check will be useful in the selection of stress levels to be specified in the application of SPDs downstream from the service entrance, from the point of view of successful cascade coordination and integrity of electromagnetic compatibility.

INCANDESCENT BULBS FAILURES

Two further experiments were conducted since the AJWG London meeting: a few 60 W, 240 V bulbs, and an arrangement of five 100 W, 120 V bulbs, each located at the end of a branch circuit of the "Upside-Down House" of increasing lengths (4,5; 9; 18; 18; 36 m). The object of the first experiment was to explore the behaviour of 240 V bulbs which was of interest to the AJWG, the object of the second to answer the question "does one bulb only fail, or do several fail in one incident when a surge impinges on the house ?".

1. Tests on bulbs rated 240 V, 60 W

These bulbs featured a clear glass, showing a horseshoe-shaped coiled filament held by the connecting stems and two auxiliary stems in a plane perpendicular to the axis of the bulb. This design is also found in some 120 V bulbs for which we had previously observed a higher flashover than that of bulbs with a straight coiled filament, typical of 120 V bulbs rated from 60 W and up. In these tests, the bulb was supplied with 240 V a.c. and positioned base down. (In my experiments conducted in the late sixties, it took a large number of bulbs to extract from the results a small correlation between base -- or filament -- orientation and failure level.)

We subjected each bulb to a Combination Wave surge, starting at 1600 V, and increasing by steps until flashover would occur. When surge flashover did occur for the first time, as indicated by the voltage measured across the lamp, it resulted in a power-frequency arc that broke the filament, the same behaviour observed for the 120 V bulbs that we tested with a Combination Wave.

Table 3 shows the results for the three bulbs that we had available. It would be interesting to determine whether the observed voltage, higher than the voltage observed for the straight-filament 120 V bulbs, is the result of the horseshoe shape, nature of the gas fill, temperature gradient in the gas around the filament, or some other design feature different from those of the 120 V bulbs. These questions are beyond the direct interest of the AJWG, but the fact remains that we have at our disposal -- if only we chose to use it -- a tool to provide a reality check on the relative frequency of occurrence of voltage surges in low-voltage a.c. circuits.

Table 3
Failure level of 240 V incandescent bulbs

Bulb sample	Peak surge required for flashover (volts)	Time to flashover (microseconds)
A	2 600	3
B	2 800	6
C	2 700	12

2. Multiple branch circuits

In this experiment, we connected a new 120 V, 100 W bulb, supplied with 120 V a.c., at the end of each of five branch circuits radiating from the service-entrance panel of our "Upside-Down House". In this manner, we sought to avoid the possibility that the bulbs surviving a surge exposure would acquire an enhanced withstand capability associated with stepping up multiple impulses, a trend that we noted in previous tests [1].

1. *Starting at low impulse levels seems to result in a higher ultimate failure level than starting at some higher level. One day, we might enlist the help of a plasma physicist and of a statistician to explore whether this apparent effect is real.*

Therefore, to conduct 16 tests, we committed 80 bulbs. Table 4 shows the results, with "X" indicating a flashover failure and "click" indicating an audible click with momentary brightening. With only one oscilloscope channel, we were unable to determine if this click was a mechanical shock of the filament or a surge flashover that did not ignite a power-frequency flashover.

Table 4
Failure of incandescent bulbs at the end of branch circuits of different lengths

Test Run	Branch circuit length (meters)				
	4,5	9	18a	18b	36
Prelim	Click		X		
A	X				
B	X				
C		X			
D		X			
E			X		
F			X		
G	X				
H		X			
I		X			
J	No flashover, click heard but not located				
K	X				
L	No flashover, click heard at 4,5 m location				
M				X	
N	X				
O				X	

From these results, it is apparent that the location of the bulb with respect to the service entrance has little to do with which fails first. Furthermore, the first one to flashover effectively protects the other bulbs. This situation should be expected, given that at 100 m/μs (round trip) the fact that the voltage of all the house is going to be clamped is established in all branch circuits by the flashover of the first bulb within the short time (less than 1 μs) necessary for the round trip of the surge and its reflected throttling. With the bulb flashovers typically occurring on the tail of the voltage wave, subsequent flashovers are prevented by the first bulb. Thus, it is the statistical distribution of the bulb flashover (if they are all of the same type) or the inherent characteristic of the bulb (of different types) that determines which goes first, not the location.

This finding can readily be applied to other devices where the mechanism of failure is an insulation breakdown. However, experience teaches us that during massive incidents of appliance failures in a residence, more than one fails. This fact points out the need to hypothesize that those multiple failures probably occur on the front of the wave rather than on the tail. This hypothesis provides another bit of information on the surge environment and appliance immunity.